

# Evaluating the Potential of a Laplacian Linear Solver

Erik G. Boman<sup>\*</sup>  
Sandia National Laboratories  
egboman@sandia.gov

Kevin Deweese<sup>†</sup>  
Department of Computer  
Science  
UC Santa Barbara  
kdeweese@cs.ucsb.edu

John R. Gilbert  
Department of Computer  
Science  
UC Santa Barbara  
gilbert@cs.ucsb.edu

## ABSTRACT

A new approach for solving Laplacian linear systems proposed by Kelner et al. involves the random sampling and update of fundamental cycles in a graph. We evaluate the performance of this approach on a variety of real world graphs. We examine different ways to choose the set of cycles and their sequence of updates with the goal of providing more flexibility and potential parallelism. We propose a parallel model of the Kelner et al. method for evaluating potential parallelism concerned with minimizing the span of edges updated at every iteration. We provide experimental results comparing the potential parallelism of the fundamental cycle basis and the extended basis. Our preliminary experiments show that choosing a non-fundamental set of cycles can save significant work compared to a fundamental cycle basis.

## 1. INTRODUCTION

### 1.1 Graph Laplacians

Networks play an important role in many application areas, including engineering, social sciences, and biology. Solving linear systems on the graph Laplacians of large unstructured networks has emerged as an important computational task in network analysis [17]. The Laplacian matrix of a weighted, undirected graph is defined as  $L = D - A$ , where  $D$  is the diagonal matrix containing the sum of incident edge weights and  $A$  is the weighted adjacency matrix. The Laplacian is symmetric and positive definite.

Most applied work on Laplacian solvers has been on preconditioned conjugate gradient (PCG) solvers, including sup-

<sup>\*</sup>Sandia is a multi-program laboratory managed and operated by Sandia Corporation, a wholly owned subsidiary of Lockheed Martin Corporation, for the U.S. Department of Energy's National Nuclear Security Administration under contract DE-AC04-94AL85000.

<sup>†</sup>Supported by Contract #618442525-57661 from Intel Corp. and Contract #DE-AC02-05CH11231 from DOE Office of Science.

port graph preconditioners [8][3][4], or specialized multigrid methods [15][14]. Spielman and Teng [18] showed how to solve these problems in nearly-linear work, later improved upon by Koutis, Miller, and Peng [13], but their algorithms do not yet have a practical implementation. An algorithm proposed by Kelner et al. [11] has the potential to solve these linear systems in nearly-linear work with a simple, implementable algorithm.

### 1.2 The Dual Randomized Kaczmarz Algorithm

The inspiration for the algorithm proposed by Kelner et al. [11], which we refer to as Dual Randomized Kaczmarz (DRK), is to treat graphs as electrical networks with resistors on the edges. For each edge, the weight is the inverse of the resistance. We can think of vertices as having an electrical potential and a net current at every vertex, and define vectors of these potentials and currents as  $v$  and  $f$  respectively. These vectors are related by the linear system  $Lv = f$ . Solving this system is equivalent to finding the set of voltages that satisfies the net "injected" currents. Kelner et al.'s DRK algorithm solves this problem with an optimization algorithm in the dual space, which finds the optimal currents on all of the edges subject to the constraint of zero net voltage around all cycles. They use Kaczmarz projections [10] to adjust currents on one cycle at a time, iterating until convergence.

We will also refer to the Primal Randomized Kaczmarz (PRK) method that applies Kaczmarz projections in the primal space [19]. One sweep of PRK performs a Kaczmarz projection with every row of the matrix. Rows are randomly permuted at every sweep.

DRK iterates over a set of *fundamental cycles*, cycles formed by adding individual edges to a spanning tree  $T$ . The fundamental cycles are a basis for the space of all cycles in the graph [7]. The resistance  $R_e$  of a cycle  $C_e$  formed by offtree edge  $e$  is defined as the sum of the resistances around the cycle

$$R_e = \sum_{e' \in C_e} r_{e'}$$

which is thought of as approximating the resistance of the offtree edge  $r_e$ . Cycles are chosen randomly, with probability  $R_e/r_e$ .

The performance of the algorithm depends on the sum of these approximate resistances, a property of the spanning tree called the *tree condition number*

$$\tau(T) = \sum_{e \in E \setminus T} \frac{R_e}{r_e}.$$

The number of iterations of DRK is proportional to the tree condition number. Kelner et al. use a particular type of spanning tree with low tree condition number, called a *low stretch tree*, specifically the one described by Abraham and Neiman [1] with  $\tau$  of  $O(m \log n \log \log n)$ . The work of one iteration is naively the cycle length, but can be reduced to  $O(\log n)$  with a fast data structure, yielding  $O(m \log n^2 \log \log n)$  total work.

### 1.3 Related Experimental Work

As the DRK algorithm is a recent and theoretical result, there are few existing implementations or performance results. Hoske et al. implemented the DRK algorithm in C++ and did timing comparisons against unpreconditioned CG on two sets of generated graphs [9]. They concluded that DRK does scale with near linear time. However, several factors make the running time too large in practice, including large tree stretch and cycle updates with unfavorable memory access patterns. They cite experimental results by Papp [16] which suggest that the theoretically low stretch tree algorithms aren't significantly better than min-weight spanning trees in practice, at least on relatively small graphs.

We also cite the experimental work of Chen and Toledo [5] on support graph preconditioners. They demonstrated that support graph preconditioners can outperform incomplete Cholesky on certain problems. There has also been some experimental work in implementing the local clustering phase of the Spielman and Teng algorithm [20].

## 2. INITIAL EVALUATION OF DRK AND COMPARISON TO PCG AND PRK

### 2.1 Experimental Design

For completeness, we include our own initial study of DRK which measures performance in terms of work instead of time, and which uses a more diverse graph test set. We implemented the algorithm in Python with Cython to see how it compared against PCG (preconditioned with Jacobi diagonal scaling) and PRK. However, we did not implement a low stretch spanning tree. Instead we use a low stretch heuristic that ranks and greedily selects edges by the sum of their incident vertex degrees (a cheap notion of centrality). We have found that this works well on unweighted graphs. We also did not implement the fast data structure Kelner et al. use to update cycles in  $O(\log n)$  work.

We do not measure wall clock time, as our DRK implementation isn't highly optimized. Instead we are interested in measuring the total work. For PCG the work is the number of nonzeros in the matrix for every iteration, plus the work of applying the preconditioner at every iteration (number of vertices for Jacobi). For PRK the work is the number of nonzero entries of the matrix for every sweep, where a sweep is a Kaczmarz projection against all the rows of  $L$ . For DRK we consider four different cost estimates for the work of updating a single cycle.

**Metric 1.** cycle length (naive)

**Metric 2.**  $\log n$  (using fast update data structure)

**Metric 3.**  $\log(\text{cycle length})$  (optimistic)

**Metric 4.** 1 (lower bound)

Updating every edge in a cycle is the naive implementation we are currently using. The data structure described by Kelner et al. can update the fundamental cycles in  $O(\log n)$  work. This may be an overestimate when the cycle length is actually less than  $\log n$ . We consider a hypothetical log of cycle length update method which we do not know to exist. However we surely cannot do better than  $O(1)$  work per cycle.

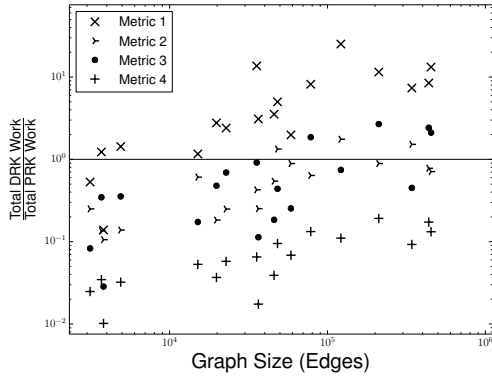
We ran experiments on all the structured mesh-like graphs and unstructured network graphs shown in Table 1. Mesh-like graphs come from more traditional applications such as model reduction and structure simulation, and contain a more regular degree distribution. Unstructured networks graphs come from electrical, road, and social networks, and contain a more irregular, sometimes exponential, degree distribution. Most of these graphs come from the UF sparse matrix collection [6]. A few 2D and 3D grids are added along with a few graphs generated with the BTER generator [12]. Weights were removed and in a few cases the matrices were symmetricized by adding the transpose. These graphs were pruned down to the largest connected component of their 2-core, by successively removing all degree 1 vertices, since DRK operates on the cycle space of the graph. The difference of the original graph and the 2-core are trees that hang off the original graph. These can be solved in linear time so we disregard them to see how solvers compare on just the structurally interesting part of the graph.

We solve to a relative residual tolerance of  $10^{-3}$ . The Laplacian matrix is singular with a nullspace dimension of one. For DRK and PRK this is not a problem but for PCG we must handle the non-uniqueness of the solution. We choose to do this by removing the last row and column of the matrix. We could also choose to orthogonalize the solution against the nullspace inside the algorithm, but we note the performance results are similar.

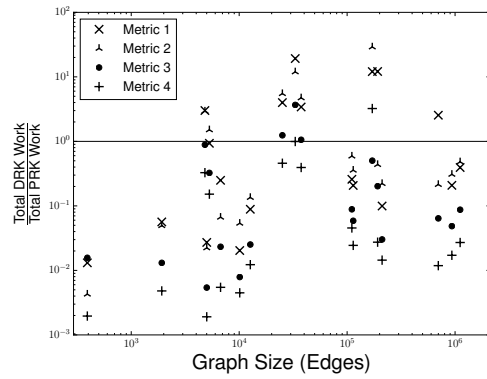
We also ran a set of PCG vs. DRK experiments where the convergence criteria is the actual error within  $10^{-3}$ . We do this knowing the solution in advance. One of the interesting results of the DRK algorithm is that, unlike PCG and PRK, convergence does not depend on the condition number of the matrix, but instead just on the tree condition number. Since higher condition number can make small residuals less trustworthy, we wondered whether convergence in the actual error yields different results.

### 2.2 Experimental Results

We compare DRK to the other solvers by examining the ratio of DRK work to the work of the other solvers. The ratio of DRK work to PRK work is plotted in Figure 1, separated by graph type. Each vertical set of four points are results for a single graph, and are sorted on the x axis by graph size. The four points represent the ratio of DRK work to PRK work under all four cost metrics. Points above the line indicate DRK performed more work while points below the line indicate DRK performed less work. Similar results for the PCG comparison are shown in Figure 2. Another set of PCG comparisons, converged to the actual error is shown in Figure 3. An example of the convergence behavior on the USpowerGrid graph is shown in Figure 4. This plot indicates how both the actual error and relative error behave during the solve for both PCG and DRK. A steeper slope indicates faster convergence. Note this only shows metric 1 work for DRK.

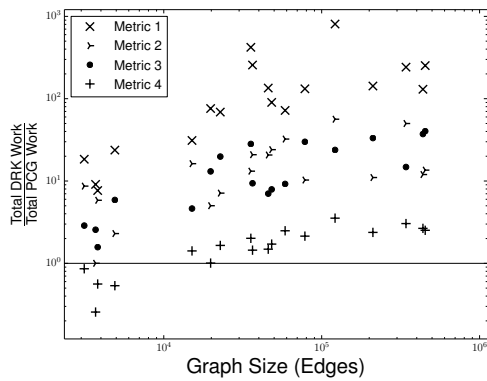


(a) Mesh-like Graphs

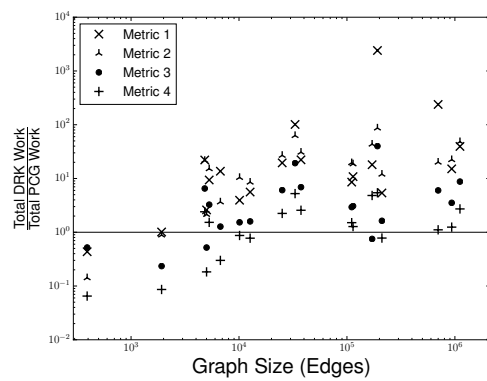


(b) Network Graphs

Figure 1: DRK vs. PRK: Relative work of DRK to PRK work under the four cost metrics is shown (PRK is better than DRK at points above the line.)

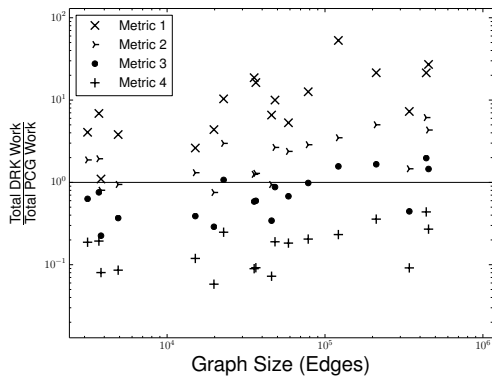


(a) Mesh Graphs

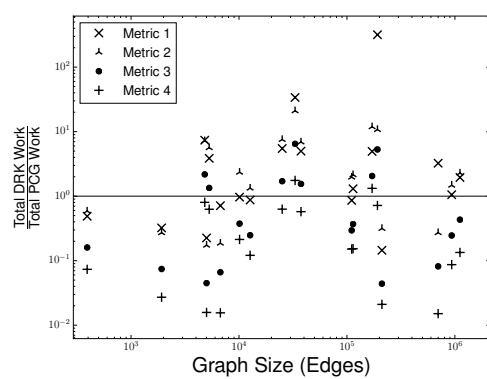


(b) Network Graphs

Figure 2: DRK vs. PCG: Relative work of DRK to PCG work under the four cost metrics is shown (PCG is better than DRK at points above the line.)



(a) Mesh Graphs



(b) Network Graphs

Figure 3: DRK vs. PCG Converged to Actual Error: Relative work of DRK to PCG work under the four cost metrics is shown, convergence tolerance is norm of actual error within  $10^{-3}$

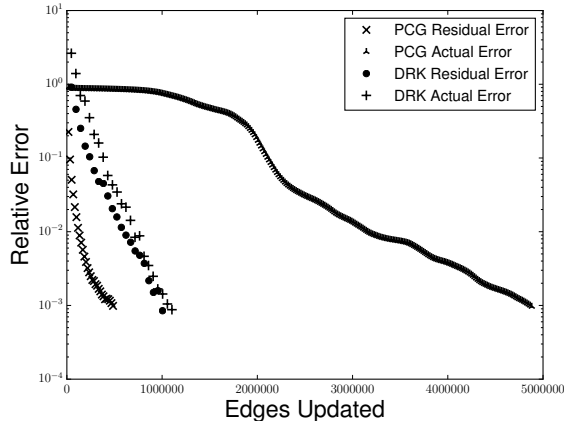


Figure 4: DRK and PCG Convergence Behavior on USpowerGrid: Relative residual error and actual error are shown for both solvers over the iterations required for convergence.

### 2.3 Experimental Analysis

In the comparison to PRK (shown in Figure 1), DRK is often better with cost metrics 3 and 4. On a few graphs, mostly networks, DRK outperforms PRK in all cost metrics (all the points are below the line.) In the comparison to PCG (shown in Figure 2), DRK fares slightly better for the network graphs, but on both graph sets these results are somewhat less than promising for. PCG often does better (most of the points are above the line.) Even if we assume unit cost for cycle updates, PCG outperforms DRK. The performance ratios also seem to get worse as graphs get larger.

The experiments concerned with the actual error (shown in Figure 3) are very interesting as they are quite different than using the residual tolerance. For all of the mesh graphs, considering the actual error makes DRK look more promising. The relative performance of cost metrics 3 and 4 are now typically better for DRK. However, PCG is still consistently better with the cost metrics 1 and 2. For some of the network graphs, the convergence behavior is similar, but for others things look much better when considering actual error. Informally the number of edges updated by DRK did not change much when switching convergence criteria, but PCG work often increased. The USpowerGrid example (shown in Figure 4) gives a sense of this. The residual error and actual error decrease similarly for DRK, but the actual error curve for PCG decreases much slower for the actual error.

## 3. NEW ALGORITHMIC IDEAS

We consider ways in which DRK could be improved by experimenting with cycles and their updates. We are in large part interested in any potential parallelism that we can take advantage of if multiple threads are used inside DRK. To this end we are interested in measuring the number of parallel steps, the longest number of steps a single thread would have to perform before convergence, maximized over all threads. We will also refer to the span, or critical path length, which is the number of parallel steps that have to be

taken if we can utilize infinite threads.

### 3.1 Expanding the Set of Cycles

Sampling fundamental cycles with respect to a tree will require updating several long cycles which will not be edge-disjoint. It would be preferable to update edge-disjoint cycles, as these updates could be done in parallel. The cycle set we use does not need to be a basis, but it does need to span the cycle space. In addition to using a cycle basis from a spanning tree, we will use several small, edge-disjoint cycles. We expect that having threads update these small cycles is preferable to having them go idle.

#### 3.1.1 2D Grid Example

We first conceived of using a different cycles basis by considering the 2D grid graph shown in Figure 5. Instead of using a tree to select cycles as in Figure 5(a) we considered using all of the face cycles. The facial cycles span the cycle space of a planar graph [7]. Half of these cycles could be updated at one iteration and then the other half could be updated during the next iteration, in a checkerboard fashion, as in Figures 5(b)(c). Furthermore, to speed up convergence, smaller cycles could be added together to form larger cycles (in a multilevel fashion) as in Figure 5(d).

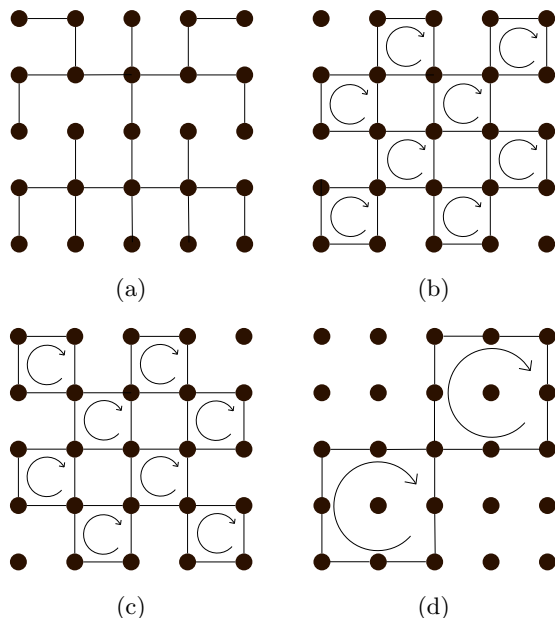


Figure 5: Grid Cycles: (a) Fundamental cycles are formed by adding edges to the spanning tree. (b-c) First level facial cycles are shown, grouped into edge-disjoint sets. (d) Second level facial cycles are formed by adding smaller facial cycles.

We implemented such a cycle update scheme using the grid face cycles, and performed experiments to see how the face cycles affected the total work measured in both the number of cycles updated (metric 4) and edges updated (metric 1). For the facial cycles, the span per iteration is the cost of updating two cycles at every level. There is no span plot for the fundamental cycles as we leave a discussion of a more general parallelization scheme to the next section. We ran experiments with and without the hierarchical combination of the face cycles against the original set

of fundamental cycles. In the case of the fundamental cycles we use H trees [2], which are known to have optimal stretch  $O(\log n)$ . Solutions were calculated to a residual tolerance of  $10^{-6}$ .

The results shown in Figure 6 indicate that the face cycles improve both the work and span. Using a hierarchical update scheme reduces the total number of edges updated. However as this requires updating larger cycles it has a worse span than simply using the lowest level of cycles.

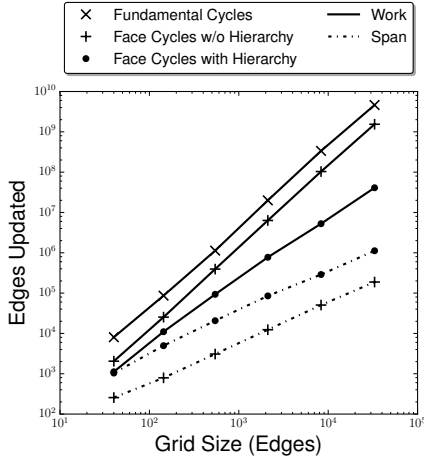


Figure 6: Grid Cycle Performance: Work and span of DRK using facial cycles and fundamental cycles are shown for two dimensional grids of various sizes.

### 3.1.2 Extension to General Graphs

The small cycles we will add to the basis we refer to as local greedy cycles. Pseudo code for finding these cycles is shown in Algorithm 1. We construct this cycle set by attempting to find a small cycle containing each edge. Starting with all edges unmarked, the algorithm selects an unmarked edge and attempts to find a path between its endpoints. This search is truncated by bounding the max number of edges searched so that each search is  $O(1)$  and constructing the entire set is  $O(m)$ . If found, this path added to the edge forms a cycle, which is added to the new cycle set, and all edges used are marked. Table 1 includes the number of local greedy cycles found for all the test graphs when the truncated BFS was allowed to search 20 edges. Greedy cycles were found on all the graphs except for the tubel graph, in which all the vertices had such large vertex degree that searching 20 edges was not enough to find a cycle.

---

#### Algorithm 1 Local Greedy Finder

---

```

function LOCAL-GREEDY(G)
  for  $e_{i,j} \in E$  do
    if  $e_{i,j}$  unmarked then
       $p_{i,j} = \text{Truncated-BFS}(G \setminus (e_{i,j}), i, j, \text{max\_edges})$ 
      Add  $p_{i,j} + e_{i,j}$  to cycle set
      Mark all edges in  $p_{i,j} + e_{i,j}$ 
    end if
  end for
end function

```

---

Adding additional cycles to the cycle basis means we also need new probabilities with which to sample all the cycles.

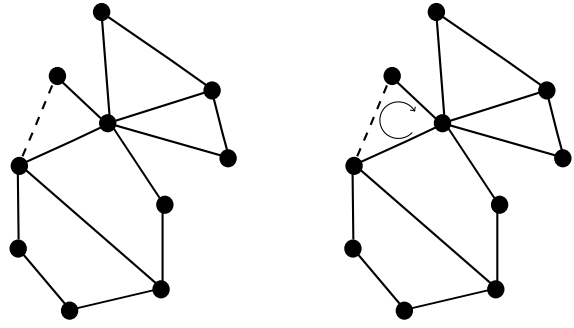


Figure 7: Local Greedy Cycles: An edge is selected on the left and a local greedy search is performed to find the cycle on the right.

Since in the unweighted case, the stretch of a cycle is just its total length, the natural choice is to update cycles proportional to their length. Though we note this might not be the best way to select cycles.

### 3.2 Cycle Sampling and Updating in Parallel

In the original DRK algorithm, cycles are chosen one at a time with probability proportional to tree stretch. We propose a parallel update scheme in which multiple threads each select a cycle. The current approach we are using is to have each thread select a cycle at every iteration with probability proportional to cycle length. If two threads select cycles that share an edge, one of the threads goes idle for that iteration. In Figure 8, threads one, two, and four select edge-disjoint cycles. However the third processor selects a cycle which contains edge 3, which is already in use by the cycle on thread 1. Processor 3 sits this iteration out while the other processors update their cycles.

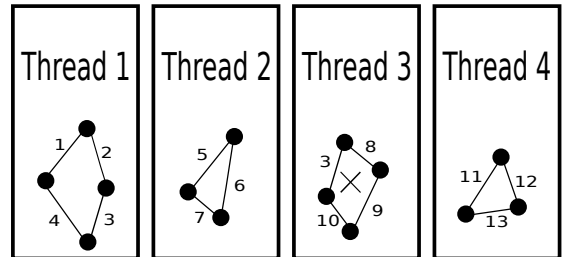


Figure 8: Example of Processors Selecting Cycles: Threads 1, 2, and 4 select edge-disjoint cycles, but thread 3 selects a cycle with edge 3 already in use. Thread 3 will go idle for an iteration.

There are various measures of parallel performance in this model that we are interested in. The first is simply the number of iterations. The second is the total work across all threads at every iteration. Lastly we are interested in the total span, or critical path length. This is the maximum of the work over all threads, summed up over all the iterations.

We envision threads working in a shared memory environment on a graph that fits in memory. This might not be realistic in practice as there must be some communication

of which edges have already been used which might be too expensive relative to the cost of a cycle update. However we are simply interested in measuring the potential parallelism, thus we ignore any communication cost.

This parallel selection scheme will change the probabilities in which cycles are selected by conditioning on edges being available  $p(C_e) = \frac{1}{\tau} \frac{R_e}{r_e} p(e' \in C_e \text{ available})$ . This selection scheme will create a bias towards smaller cycles with less conflicting edges as more threads are added, which can increase total work.

## 4. EXPERIMENTS AND RESULTS

### 4.1 Experimental Design

We performed experiments on a variety of unweighted graphs from the UF Sparse Matrix Collection (the same test set as in Section 2, shown in Table 1). Again we distinguish between structured mesh-like graphs and unstructured network graphs.

We continue to use our Python/Cython implementation of DRK, without a low stretch spanning tree or a cycle update data structure. The code does not run in parallel, but we simulate parallelism on multiple threads by selecting and updating edge-disjoint cycles at every iteration as described above.

Our experiments consist of two sets of strong scaling experiments, the spanning tree cycles with and without local greedy cycles, up to 32 threads. We set a relative residual tolerance of  $10^{-3}$ . We consider the same 4 cycle update cost metrics as used in the PCG comparisons in Section 2: cycle length,  $\log n$ ,  $\log(\text{cycle length})$ , and unit cost. However in the case of the local greedy cycles, which cannot use the  $\log n$  update data structure, and we always just charge the number of edges in a cycle. For all the work cost models, we measure the total work required for convergence and the number of parallel steps taken to converge. For metric 4 these will be the same. A condensed subset of the scaling results are shown in Table 2.

### 4.2 Experimental Results

We first examine the effects of using a different cycle basis sequentially. We estimate the usefulness of extra cycles as the length of the largest cycle in the fundamental set normalized by the number of cycles in the fundamental set. This is because we suspect the large cycles to be a barrier to performance as they are updated the most frequently, and at higher cost depending on the cost metric. We plot the performance of the local greedy cycles on the two different graph types (shown on the highest and lowest cost metrics in Figure 9). These figures show the ratio between the work of the different cycle sets as a function of the estimated usefulness. Points below the line indicate that adding the local greedy cycles improved performance.

Figure 10 shows examples of our results on three of the graphs. In Figure 10(a) the parallel steps (with the four different metrics) is plotted as a function of the number of threads used for the barth5 graph. The total edge cost is cost at the top of the plot, while the unit cost is at the bottom. These results are shown for both sets of cycles, with and without local greedy. Figure 11 shows the effect of adding threads to the total work.

To measure the parallel performance across multiple graphs we will look at the average speedup of the span metrics

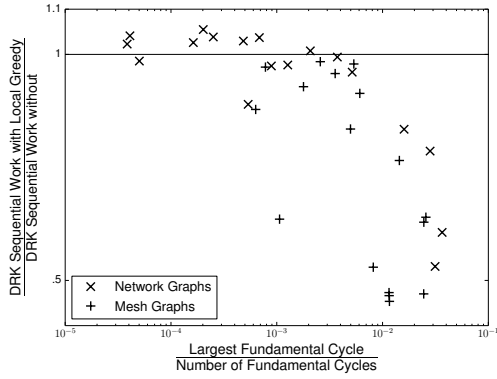
across all graphs. Speedup is defined as the sequential work of one thread over the number of parallel steps on multiple threads. The speedup with and without cycles is shown in Figure 12. Note that without local greedy cycles metric 2 and metric 4 speedup are the same as the costs differ by  $\log n$ . We compare the speedup between the different cycle sets for the different graph types in Figure 13. The speedup of using 8 threads without local greedy is plotted against the speedup of using 8 threads with local greedy.

### 4.3 Experimental Analysis

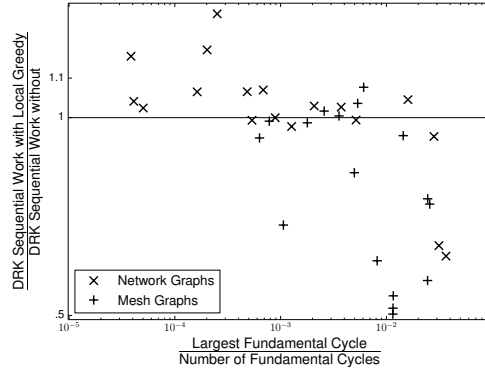
In the serial results shown in Figure 9 we see that our usefulness estimate is a crude guess at when local greedy cycles will be helpful. There seems to be a threshold of largest cycle length over which local greedy cycles can be useful, but under which there's not much difference. Also note that meshes tend to have larger, largest cycles than networks, leading to local greedy cycles working better on meshes. The local greedy cycle improvement is slightly better metric 1 where we count every edge update. At the other extreme, when updating large cycles is the same cost (unit) as small cycles added by local greedy, the local cycles are less effective. However there is still an improvement in number of cycles updated. We tried but were unable to find some measure of the usefulness of a single local greedy cycle.

The parallel steps scaling of the mesh-like barth5 graph (shown in Figure 10(a)) is an example of the local greedy cycles improving both sequential performance and scaling performance. At the left of this plot we see the extra cycles improve results sequentially. Then as threads are added parallel the steeper slope indicates the local greedy cycles improved parallel steps scaling. The parallel steps scaling of the mesh-like tuma1 graph (shown in Figure 10(b)) is an example of the local greedy cycles improving sequential performance, but with similar or worse scaling. At the left of this plot we see the extra cycles improve results sequentially, but when scaled to 32 threads performance is similar. The parallel steps scaling of the network email graph (shown in Figure 10(c)) is an example in which the local greedy cycles do not improve sequential performance, and scaling is poor with both cycle sets. There is little difference between the different cycle sets in this plot. Furthermore scaling is poor and quickly flattens out by about four threads. For a better understanding of the poor parallel steps scaling we examine the total work scaling (shown in Figure 11, showing how much extra work we have to do when skewing the probability distribution. This extra work quickly increases, limiting the parallel performance.

In the speedup plot (shown in Figure 12), we see similar speedup for both cycle sets. On mesh graphs the local greedy cycles do slightly better on all cost metrics beyond 16 threads. However on the network graphs, only with cycle cost metric 4 do the local greedy cycles perform better, and under metric 3 they perform worse. (Again note that without local greedy cycles metric 4 and metric 3 speedups are the same.) We hypothesized that giving the solver smaller, extra cycles would improve the parallel performance compared to the fundamental cycles. However this seems to only be true for mesh like graphs, and even then the improvement is minimal. An interesting thing to note is that the speedup is better with the  $\log n$  cost model. This is probably due to overcharging small cycles, which is less of an issue when there are more threads to pick potentially

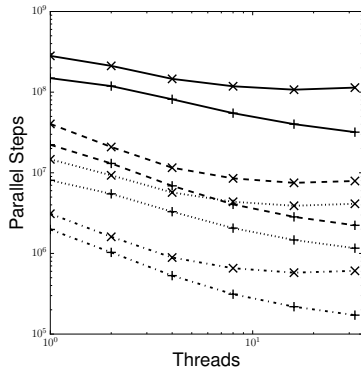


(a) Metric 1

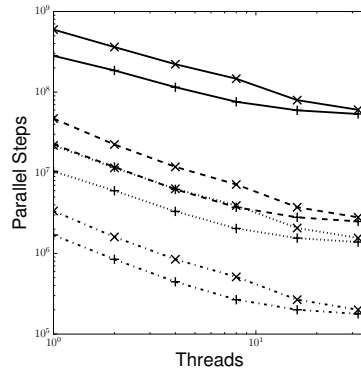


(b) Metric 4

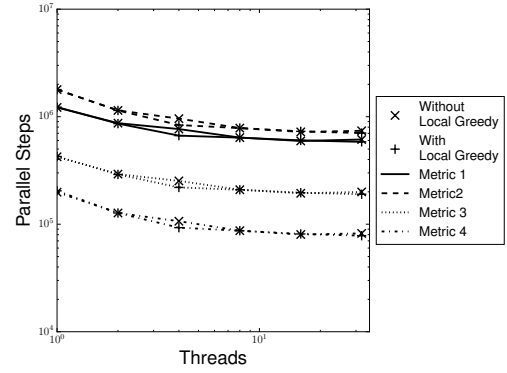
Figure 9: Sequential Comparison of Cycle Set Work: The ratio of DRK work with local greedy cycles to DRK without local greedy on one thread is plotted against an estimate of the usefulness of extra cycles (local greedy performed better below the line.)



(a) barth5



(b) tuma1



(c) email

Figure 10: Parallel Steps Scaling (shown for three example graphs): As threads are added, parallel steps decreases for both cycle sets (steeper slope indicates better scaling)

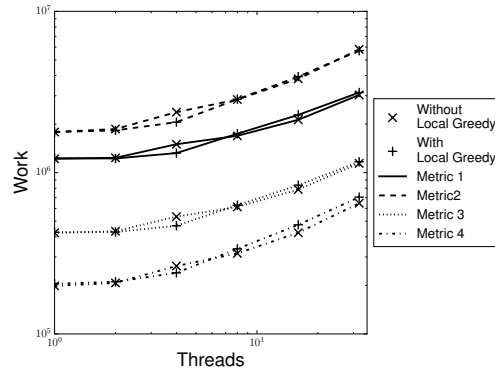


Figure 11: Total Work Scaling of email Graph: As threads are added the total work increases for both cycle sets (ideally it would stay constant).

larger cycles. Taking a snapshot of these results on eight threads (shown in Figure 13), we see that there are some

networks graphs which don't have much speedup for either cycle set (bottom left of the plot). However there are meshes

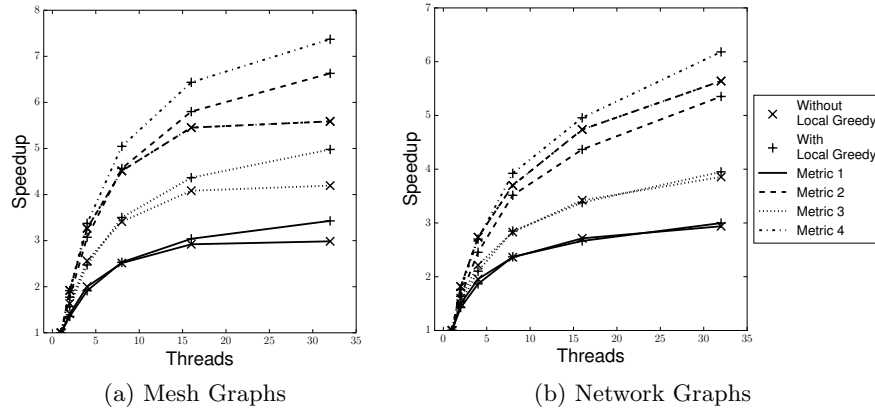


Figure 12: Average Parallel Steps Speedup: The ratio of sequential work on one thread to parallel steps on multiple threads is plotted up to 32 threads.

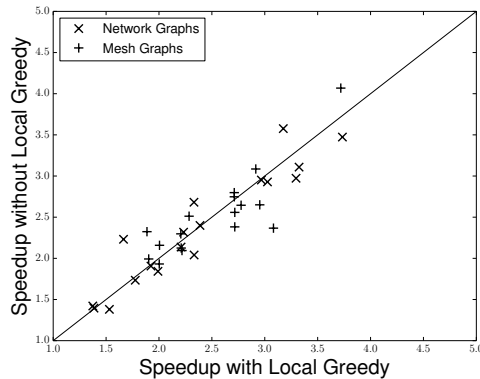


Figure 13: 8 Thread Speedup Comparison: The ratio of the 8 thread speedups of both cycle sets are plotted for all graphs (below the line local greedy speedup is better).

and networks which enjoy a speedup for both cycle sets (top right of the plot). It's difficult to say on what graphs could using different cycles aid with parallelism.

## 5. CONCLUSIONS

We have done an initial comparison of Kelner et al.'s DRK with PCG and PRK. These results, which simply measure algorithm work by number of edges touched, do not at present support the practical utility of DRK. For mesh-like graphs, PCG usually takes less work than DRK, even if DRK is charged only one unit of work per cycle update. This suggests that the fast cycle update data structure proposed by Kelner et al. (or any undiscovered fast update method) will not be enough to provide practical utility to DRK. It does seem that DRK is an improvement to PRK on several graphs, mostly networks. One promising result of these experiments is that DRK converges to small actual error similarly to residual error, while PCG sometimes does not. More PCG iterations are required when solving to a low actual error, while DRK work does not increase very much. More work should be done to understand this behavior.

The experiments in this paper were limited to unweighted graphs for simplicity. Experiments with weighted graphs

should be run for more complete results. An open question is whether there is a class of graphs with high condition number, but with practical low stretch trees where DRK will perform asymptotically better.

We suggest techniques for improving DRK in practice. We consider using a non fundamental cycle basis to accelerate convergence. Using face cycles of a two-dimensional grid graph greatly reduces the required number of edge updates compared to the fundamental cycle basis. We attempt to generalize these cycles by finding small local greedy cycles. We found these cycles can accelerate convergence, especially for mesh like graphs. Because of the randomized nature of DRK, it is difficult to measure the usefulness of any one cycle in the basis, so it is difficult to determine where and which extra cycles are useful.

We also consider how DRK could be implemented in parallel to take advantage of simultaneous updates of edge disjoint cycles. We describe a model in which threads select cycles, and go idle if a conflicting edge is found. While this can increase total work, we find this can often reduce the number of parallel steps. However there is a limit to this parallelism. Furthermore, this scaling behavior seems to be very similar with or without local greedy cycles.



## 6. REFERENCES

- [1] I. Abraham and O. Neiman. Using petal-decompositions to build a low stretch spanning tree. In *Proceedings of the 45th annual ACM Symp. on Theory of Comp.*, pages 395–406. ACM, 2012.
- [2] N. Alon, R. M. Karp, D. Peleg, and D. West. A graph-theoretic game and its application to the k-server problem. *SIAM Journal on Computing*, 24(1):78–100, 1995.
- [3] M. Bern, J. Gilbert, B. Hendrickson, N. Nguyen, and S. Toledo. Support-graph preconditioners. *SIAM Journal Matrix Anal. Appl.*, 27(4):930–951, 2006.
- [4] E. G. Boman, D. Chen, B. Hendrickson, and S. Toledo. Maximum-weight-basis preconditioners. *Numerical Linear Algebra Appl.*, 11:695–721, 2004.
- [5] D. Chen and S. Toledo. Vaidya’s preconditioners: Implementation and experimental study. *ETNA. Electronic Transactions on Numerical Analysis [electronic only]*, 16:30–49, 2003.
- [6] T. A. Davis and Y. Hu. The University of Florida Sparse Matrix Collection. *ACM Transactions on Mathematical Software*, 38(1):1:1–1:25, Nov. 2011.
- [7] R. Diestel. *Graph Theory*, volume 173, pages 23–28. Springer, 2012.
- [8] K. Gremban. *Combinatorial Preconditioners for Sparse, Symmetric, Diagonally Dominant Linear Systems*. PhD thesis, Carnegie Mellon University, Pittsburgh, October 1996.
- [9] D. Hoske, D. Lukarski, H. Meyerhenke, and M. Wegner. Is nearly-linear the same in theory and practice? A case study with a combinatorial laplacian solver. *Computing Research Repository*, abs/1502.07888, 2015.
- [10] S. Kaczmarz. Angenäherte auflösung von systemen linearer gleichungen. *Bulletin International de l’Academie Polonaise des Sciences et des Lettres*, 35:355–357, 1937.
- [11] J. A. Kelner, L. Orecchia, A. Sidford, and Z. A. Zhu. A simple, combinatorial algorithm for solving SDD systems in nearly-linear time. In *Proceedings of the 45th ACM Symp. Theory of Comp. (STOC ’13)*, pages 911–920, New York, 2013.
- [12] T. G. Kolda, A. Pinar, T. Plantenga, and C. Seshadhri. A scalable generative graph model with community structure. *SIAM Journal on Scientific Comp.*, 36(5):C424–C452, 2014.
- [13] I. Koutis, G. L. Miller, and R. Peng. Approaching optimality for solving SDD systems. *Computing Research Repository*, abs/1003.2958, 2010.
- [14] I. Koutis, G. L. Miller, and D. Tolliver. Combinatorial preconditioners and multilevel solvers for problems in computer vision and image processing. *Computer Vision and Image Understanding*, 115(12):1638 – 1646, 2011.
- [15] O. E. Livne and A. Brandt. Lean algebraic multigrid (LAMG): Fast graph Laplacian linear solver. *SIAM Journal on Scientific Comp.*, 34(4):B499–B522, 2012.
- [16] P. A. Papp. Low-stretch spanning trees. Undergraduate thesis, Eötvös Loránd University, 2014.
- [17] D. A. Spielman. Algorithms, graph theory, and linear equations in Laplacian matrices. In *Proceedings of the International Congress of Mathematicians*, volume 4, pages 2698–2722, 2010.
- [18] D. A. Spielman and S. Teng. Nearly-linear time algorithms for graph partitioning, graph sparsification, and solving linear systems. In *Proceedings of the 36th Annual ACM Symp. on Theory of Comp.*, STOC ’04, pages 81–90, New York, NY, USA, 2004. ACM.
- [19] T. Strohmer and R. Vershynin. A randomized Kaczmarz algorithm with exponential convergence. *Journal of Fourier Analysis and Applications*, 15(2):262–278, 2009.
- [20] Z. A. Zhu, S. Lattanzi, and V. S. Mirrokni. A local algorithm for finding well-connected clusters. *Computing Research Repository*, abs/1304.8132, 2013.

Graph (Collection)	Nodes	Edges	2-core Nodes	2-Core Edges	Greedy Cycles	Probability of Selecting Greedy	Largest Cycle Length
jagmesh3 (HB)	1.09k	3.14k	1.09k	3.14k	1.92k	0.2419	77
lshp1270 (HB)	1.27k	3.70k	1.27k	3.70k	2.17k	0.4712	95
rail_1357 (Oberwolfach)	1.36k	3.81k	1.36k	3.81k	1.85k	0.2507	55
50 x 50 grid	2.50k	4.90k	2.50k	4.90k	2.40k	0.5000	120
data (DIMACS10)	2.85k	15.1k	2.85k	15.1k	7.43k	0.1760	92
100 x 100 grid	10.0k	19.8k	10.0k	19.8k	9.80k	0.5000	230
20 x 20 x 20 grid	8.00k	22.8k	8.00k	22.8k	3.57k	0.1941	122
L-9 (A-G Monien)	18.0k	35.6k	18.0k	35.6k	17.6k	0.4992	411
tuma1 (GHS_indef)	23.0k	37.2k	22.2k	36.5k	10.7k	0.0610	420
barth5 (Pothen)	15.6k	45.9k	15.6k	45.9k	29.9k	0.1765	375
cti (DIMACS10)	16.8k	48.2k	16.8k	48.2k	7.27k	0.0501	172
aft01 (Okunbor)	8.21k	58.7k	8.21k	58.7k	26.6k	0.6680	105
30 x 30 x 30 grid	27.0k	78.3k	27.0k	78.3k	8.35k	0.1399	202
wing (DIMACS10)	62.0k	122k	62.0k	122k	27.9k	0.0301	605
olesnik0 (GHS_indef)	88.3k	342k	88.3k	342k	220k	0.1327	363
tube1 (TKK)	21.5k	438k	21.5k	438k	0	0.0000	102
fe.tooth (DIMACS10)	78.1k	453k	78.1k	453k	217k	0.3673	286
dawson5 (GHS_indef)	51.5k	480k	20.2k	211k	19.8k	0.0941	165

(a) Structured Mesh-like Graphs

Graph (Collection)	Nodes	Edges	2-core Nodes	2-core Edges	Greedy Cycles	Probability of Selecting Greedy	Largest Cycle Length
EVA (Pajek)	8.50k	6.71k	314	492	84	0.2346	18
bcsprw09 (HB)	1.72k	2.40k	1.25k	1.92k	651	0.3276	54
BTER1 $d_{avg} = 10, d_{max} = 30$ $cc_{max} = .3, cc_{global} = .1$	981	4.85k	940	4.82k	510	0.0465	18
USpowerGrid (Pajek)	4.94k	6.59k	3.35k	5.01k	1.68k	0.2997	80
email (Arenas)	1.13k	5.45k	978	5.30k	362	0.0433	11
uk (DIMACS10)	4.82k	6.84k	4.71k	6.72k	1.97k	0.2488	211
as-735 (SNAP)	7.72k	13.9k	4.02k	10.1k	3.83k	0.0822	9
ca-GrQc (SNAP)	4.16	13.4k	3.41k	12.7k	4.43k	0.2315	22
BTER2 $d_{avg} = 10, d_{max} = 70$ $cc_{max} = .3, cc_{global} = .1$	4.86k	25.1k	4.54k	24.8k	2.69k	0.0468	17
gemat11 (HB)	4.93k	33.1k	4.93k	33.1k	9.72k	0.0011	42
BTER3 $d_{avg} = 15, d_{max} = 70$ $cc_{max} = .6, cc_{global} = .15$	4.94k	37.5k	4.66k	37.2k	4.79k	0.0518	18
dictionary28 (Pajek)	52.7k	89.0k	20.9k	67.1k	20.2k	0.1410	36
astro-ph (SNAP)	16.7k	121k	11.6k	111k	13.2k	0.0786	18
cond-mat-2003 (Newman)	31.2k	125k	25.2k	114k	32.5k	0.1533	23
BTER4 $d_{avg} = 15, d_{max} = 30$ $cc_{max} = .6, cc_{global} = .15$	999	171k	999	171k	33	0.0002	7
HTC_336_4438 (IPSO)	226k	339k	64.1k	192k	32.9k	0.0339	990
OPF_10000 (IPSO)	43.9k	212k	42.9k	211k	122k	0.3146	53
ga2010 (DIMACS10)	291k	709k	282k	699k	315k	0.1466	941
coAuthorsDBLP (DIMACS10)	299k	978k	255k	934k	297k	0.1524	36
citationCiteseer (DIMACS10)	268k	1.16M	226k	1.11M	150k	0.0484	56

(b) Unstructured Network Graphs

Table 1: Statistics of All Graphs Used in Experiments

Graph and Metric	Sequential Work (with Local Greedy)	2 Thread Parallel Steps (with Local Greedy)	8 Thread Parallel Steps (with Local Greedy)
jagmesh3 (Metric 1)	2.73M (1.72M)	2.02M (1.26M)	1.07M (28.3K)
jagmesh3 (Metric 4)	127K (101K)	69.7K (51.2K)	632K (17.4K)
lshp1270 (Metric 1)	6.80M (4.35M)	4.87M (3.50M)	3.41M (2.29M)
lshp1270 (Metric 4)	192K (150K)	104K (85.1K)	61.0K (41.9K)
rail1357 (Metric 1)	1.64M (1.26M)	1.21M (909K)	653K (550K)
rail1357 (Metric 4)	119K (114K)	63.8K (57.0K)	143K (143K)
50 x 50 grid (Metric 1)	9.42M (4.32M)	9.42M (4.43M)	3.55M (1.50M)
50 x 50 grid (Metric 4)	213K (125K)	115K (62.5K)	45.0K (20.0K)
data (Metric 1)	17.9M (16.4M)	13.1M (13.1M)	8.43M (7.41M)
data (Metric 4)	815K (878K)	416K (470K)	185K (168K)
100 x 100 grid (Metric 1)	84.0M (38.1M)	59.7M (29.1M)	27.2M (13.1M)
100 x 100 grid (Metric 4)	1.11M (610K)	560K (310K)	180K (90.0K)
20 x 20 x 20 grid (Metric 1)	64.7M (63.3M)	45.3M (46.0M)	30.9M (28.6M)
20 x 20 x 20 grid (Metric 4)	1.55M (1.61M)	816K (856K)	448K (416K)
L-9 (Metric 1)	820M (382M)	557M (266M)	346M (124M)
L-9 (Metric 4)	3.92M (2.03M)	2.07M (1.04M)	1.10M (396K)
tuma1 (Metric 1)	597M (282M)	362M (186M)	147M (75.9M)
tuma1 (Metric 4)	3.36M (1.69M)	1.60M (845K)	512K (267K)
barth5 (Metric 1)	282M (149M)	212M (119M)	118M (54.9M)
barth5 (Metric 4)	3.11M (1.98M)	1.61M (1.03M)	655K (312K)
cti (Metric 1)	204M (195M)	142M (143M)	87.7M (103M)
cti (Metric 4)	3.87M (3.89M)	2.02M (2.09M)	1.01M (1.20M)
aft01 (Metric 1)	127M (118M)	90.8M (88.3M)	45.4M (43.5M)
aft01 (Metric 4)	4.38M (4.32M)	2.19M (2.22M)	763k (738k)
30 x 30 x 30 grid (Metric 4)	401M (394M)	284M (283M)	152M (142M)
30 x 30 x 30 grid (Metric 4)	6.51M (6.62M)	3.35M (3.40M)	1.35M (1.27M)
wing (Metric 1)	4.98B (4.16B)	3.41B (2.99B)	2.58B (2.08B)
wing (Metric 4)	21.8M (18.8M)	12.2M (10.8M)	8.31M (6.70M)
olesnik0 (Metric 1)	2.69B (1.71B)	1.99B (1.36B)	978M (630M)
olesnik0 (Metric 4)	33.8M (24.6M)	16.9M (1.28M)	5.47M (3.62M)
tubel (Metric 1)	2.74B (N/A)	1.98B (N/A)	1.59B (N/A)
tubel (Metric 4)	56.1M (N/A)	32.0M (N/A)	22.9M (N/A)
fe_tooth (Metric 1)	6.56B (5.76B)	4.46B (4.09B)	3.04B (2.87B)
fe_tooth (Metric 4)	65.5M (62.1M)	34.3M (32.7M)	19.8M (18.8M)
dawson5 (Metric 1)	1.49B (1.45B)	1.06B (1.05B)	650M (658M)
dawson5 (Metric 4)	24.9M (24.7M)	12.8M (12.8M)	6.11M (6.19M)

(a) Structured Mesh-like Graphs

Graph and Metric	Sequential Work (with Local Greedy)	2 Thread Parallel Steps (with Local Greedy)	8 Thread Parallel Steps (with Local Greedy)
EVA (Metric 1)	41.4K (25.1K)	22.5K (23.8K)	18.5K (15.1K)
EVA (Metric 4)	6.28K (4.08K)	2.83K (3.14K)	1.88K (1.88K)
bcspwr09 (Metric 1)	308K (242K)	199K (165K)	130K (115K)
bcspwr09 (Metric 4)	26.2K (24.9K)	12.5K (12.5K)	4.99K (4.99K)
BTER1 (Metric 1)	2.26M (2.25M)	1.78M (1.76M)	1.59M (1.64M)
BTER1 (Metric 4)	246K (253K)	243K (253K)	333K (397K)
USpowerGrid (Metric 1)	1.06M (887K)	735K (557K)	297K (279K)
USpowerGrid (Metric 4)	73.8K (77.1K)	36.9K (33.5K)	10.1K (10.1K)
email (Metric 1)	1.22M (1.23M)	871K (862K)	639K (638K)
email (Metric 4)	199K (204K)	127K (127K)	87.0K (87.0K)
uk (Metric 1)	7.30M (3.88M)	5.51M (3.29M)	3.04M (1.62M)
uk (Metric 4)	160K (108K)	84.8K (61.2K)	33.0K (18.8K)
as-735 (Metric 1)	911K (887K)	498K (500K)	293K (267K)
as-735 (Metric 4)	201K (201K)	96.6K (109K)	48.3K (44.2K)
ca-GrQc (Metric 1)	2.98M (3.39M)	1.92M (2.16M)	923K (950K)
ca-GrQc (Metric 4)	413K (509K)	201K (242K)	71.7K (75.1K)
BTER2 (Metric 1)	11.3M (11.7M)	8.21M (8.31M)	6.52M (6.60M)
BTER2 (Metric 4)	1.30M (1.39M)	876K (894K)	658K (667K)
gemat11 (Metric 1)	63.7M (62.2M)	50.4M (49.4M)	45.7M (44.9M)
gemat11 (Metric 4)	3.30M (3.22M)	2.38M (2.33M)	2.07M (2.04M)
BTER3 (Metric 1)	18.5M (19.0M)	14.6M (14.1M)	13.4M (12.4M)
BTER3 (Metric 4)	2.13M (2.27M)	1.59M (1.54M)	1.39M (1.29M)
dictionary28 (Metric 1)	38.0M (33.8M)	24.4M (24.6M)	16.4M (15.2M)
dictionary28 (Metric 4)	3.20M (3.18M)	1.65M (1.78M)	941K (878K)
astro-ph (Metric 1)	25.3M (25.9M)	15.7M (16.3M)	8.63M (8.57M)
astro-ph (Metric 4)	4.45M (4.74M)	2.27M (2.43M)	1.01M (1.01M)
cond-mat-2003 (Metric 1)	38.8M (40.9M)	27.4M (30.3M)	21.0M (20.5M)
cond-mat-2003 (Metric 4)	4.57M (5.35M)	2.62M (3.10M)	1.74M (1.72M)
BTER4 (Metric 1)	25.4M (26.4M)	15.1M (15.1M)	8.53M (8.01M)
BTER4 (Metric 4)	6.78M (7.06M)	3.67M (3.67M)	1.84M (1.73M)
HTC_336_4438 (Metric 1)	14.2B (13.7B)	8.50B (8.89B)	4.10B (3.67B)
HTC_336_4438 (Metric 4)	32.2M (32.0M)	15.9M (16.9M)	6.80M (6.09M)
OPF_10000 (Metric 1)	47.3M (49.1M)	31.8M (33.2M)	16.0M (16.5M)
OPF_10000 (Metric 4)	6.86M (8.66M)	3.34M (4.29M)	857K (1.07M)
ga2010 (Metric 1)	8.77B (6.16B)	6.88B (4.97B)	3.21B (2.59B)
ga2010 (Metric 4)	40.8M (33.5M)	20.8M (16.9M)	6.48M (5.35B)
coAuthorsDBLP (Metric 1)	539M (552M)	356M (371M)	264M (237M)
coAuthorsDBLP (Metric 4)	44.4M (51.3M)	23.5M (26.3M)	15.3M (13.8M)
citationCiteseer (Metric 1)	1.08B (1.07B)	716M (723M)	506M (482M)
citationCiteseer (Metric 4)	74.4M (76.2M)	40.7M (41.8M)	25.3M (24.2M)

(b) Unstructured Network Graphs

Table 2: Condensed Results of Scaling Experiments